Enhanced plastic deformation ability of copper matrix composites through synergistic strengthening of nano-Al2O3 and Cr particles

GUO, Xiuhua, XU, Guoyang, LI, Shaolin, SONG, Kexing, LIU, Song, WANG, Xu, LUO, Quanshun <http://orcid.org/0000-0003-4102-2129>, LIU, Haitao and SONG, Hao

Published version

GUO, Xiuhua, XU, Guoyang, LI, Shaolin, SONG, Kexing, LIU, Song, WANG, Xu, LUO, Quanshun, LIU, Haitao and SONG, Hao (2024). Enhanced plastic deformation ability of copper matrix composites through synergistic strengthening of nano-Al2O3 and Cr particles. Materials Science and Engineering: A, 910: 146886.

Enhanced plastic deformation ability of copper matrix composites through synergistic strengthening of nano-Al_2O_3 and Cr particles

Xiuhua Guo [a], Guoyang Xu [a], Shaolin Li [a], Kexing Song [a,b] *, Song Liu [a], Xu Wang [a], Quanshun Luo[c], Haitao Liu [a], Hao Song [a]

[a] *School of Materials Science and Engineering, Henan Key Laboratory of Non-ferrous Materials Science and Processing Technology, Henan University of Science and Technology, Luoyang 471023, China*

[b] *Henan Key Laboratory of Advanced Conductor Materials, Henan Academy of Sciences, Zhengzhou 450046, China*

c. Materials and Engineering Research Institute, Sheffield Hallam University, Sheffield S1 1WB, UK

* Corresponding author.

E-mail addresses: kxsong@haust.edu.cn (Kexing Song)

Abstracts: The commercial application of Al_2O_3/Cu composites (ODS copper) with high Al_2O_3 content is consistently restricted by their plastic deformability. In order to synergistically improve the plastic deformability of Al_2O_3/Cu composites, Al_2O_3/Cu-Cr composites with different Cr contents are prepared by internal oxidation combined with heat treatment by replacing part of the Al_2O_3 particles with Cr phases heat treatment. The effects of Cr content on the microstructure and plastic deformability of Al_2O_3/Cu-Cr composites are investigated. It is found that the nano-Al_2O_3 (8 nm) and Cr (25 nm) particles are uniformly distributed in the copper matrix, and both reach a semi-congruent interface with copper matrix. Meanwhile, the copper matrix undergoes a transition from a $[111]_{Cu}$ hard orientation to a $[100]_{Cu}$ soft orientation, and the increase in Cr content leads to a more pronounced degree of recrystallization in the Al_2O_3/Cu-Cr composites. The results of geometric phase analysis (GPA) show that the coordinated deformability between Cr and Cu is better than that between Al_2O_3 and Cu. The elongation of 2.5Al_2O_3/Cu-0.3Cr composite increased to 24.48% from 22.47% of the Cr-free 2.8Al_2O_3/Cu composite. The results of tensile strength calculations show that the tensile strength of Al_2O_3/Cu-Cr composites is mainly dominated by matrix strengthening and Orowan strengthening induced by Al_2O_3 particles, while grain strengthening, dislocation strengthening, and Orowan strengthening induced by Cr particles play a secondary role. The correlation coefficient (R^2) is 0.95 after fitting the experimental and theoretical values of tensile strength of Al_2O_3/Cu-Cr composites.

Keywords: Al_2O_3/Cu-Cr composites, Plastic deformability, Aging treatment, Recrystallization, Strengthening mechanisms

1. Introduction

Al_2O_3/Cu composites (oxide dispersion strengthened copper or ODS copper) prepared by internal oxidation method have the combined excellent conductivity and good mechanical properties at elevated temperatures due to the diffuse distribution of nano-Al_2O_3 particles in the copper matrix. The composites are widely used in circuit package components, electrical contact components, bias filter walls of thermonuclear reactor, etc. [1-3]. However, the contradiction between the improving mechanical properties and weakening plastic deformability is prevalent in metal matrix composites induced by the addition of reinforcing phases [4-5].

In Al_2O_3/Cu composites, the interfacial occupancy between Al_2O_3 and Cu increases with increasing Al_2O_3 content, whereas strong interactions between the Al_2O_3 particles and the dislocations in the Cu matrix during the deformation process bring about interfacial stress concentrations leading to reduced plastic deformability [6-8]. For example, Chen et al. [9] found that the tensile strength of Al_2O_3/Cu composites increased with increasing Al_2O_3 content at the expense of gradually decreased elongation. Hence, the industrial production of Al_2O_3/Cu composites with high Al_2O_3 content is severely restricted because of the deformation difficulties and cracking during the densification process [10-11]. Therefore, how to improve the plastic deformability without significant loss of the mechanical properties remains as a challenge in the production of Al_2O_3/Cu composites.

In recent years, researchers have focused on improving the plastic deformability of Al_2O_3/Cu composites by optimizing the preparation process and the design of the material components[12-13]. For instance, Dong et al. [14] investigated the effects of hot extrusion and hot rolling on the plastic deformability of Cu-5 vol.% Al_2O_3 composite. It was found that the elongation of Al_2O_3/Cu composite after hot extrusion and hot rolling was by 7% higher than after hot extrusion alone, while the tensile strength decreased slightly. Mukhtara et al. [15] investigated the influence of the forging process on the properties of pure Cu and Al_2O_3/Cu composites. It was found that the plastic deformability of Al_2O_3/Cu composites was significantly reduced compared to pure Cu. Zhang et al. [16] found that incorporating trace amount (0.02 wt%) of La improved the elongation of Cu-0.5wt%Al_2O_3 composites by 3.4% and the ultimate tensile strength by 74 MPa. In addition, according to binary alloy theory, solutioning and aging treatments can also be used to strengthen copper matrix composites, such as the introduction of less soluble alloying elements such as Cr, Zr, Ti, etc. [17-18]. Diao et al. found that the elongation of Cu-0.5 wt.%Cr-0.02 wt.%Zr alloy increased by 9.2% after solutioning and aging treatment compared to direct aging treatment, while the tensile strength increased by 63 MPa [19] . Zhang et al. reported that the incorporation of Ti improved the interfacial strength between Al_2O_3 and Cu, resulting in a 3.6% increase in elongation of Cu-2.03 wt.%Al_2O_3-0.2 wt.%Ti compared to Cu-2.03 wt.%Al_2O_3 [20].

The present work aims to study the feasibility of improving the plastic deformability of Al_2O_3/Cu composites by introducing Cr particles while maintaining their strength of composite. Al_2O_3/Cu-Cr composites with various Cr contents were fabricated by internal oxidation and heat treatment methods, followed by experimental investigations of the microstructure, electrical conductivity, mechanical properties, plastic deformability and strengthening mechanisms. The results will support new studies to improve the plasticity of copper matrix composites.

2. Experimental procedures

2.1. Raw materials

The raw materials were Cu-0.6 wt.%Al alloy powder (99.9% purity, supplied by Hunan Finepowd Materials Co., Ltd, 45μm), Cu-1.5wt.%Cr alloy powder (99.99% purity, supplied by Nangong Cockin Welding Materials Co., Ltd, 35μm) and Cu_2O powder (99.99% purity, supplied by Shanghai Xiangtian Nanomaterials Co., Ltd, 1μm). The theoretical overall volume fraction of in-situ generated Al_2O_3 in the Cu-Al-Cr-O system is 2.8%. To ensure complete in-situ reaction, the actual amount of Cu_2O is the product of the oxygen source factor and the mass ratio of chemical equation, where the oxygen source factor is 1 [21]. The compositions of the Al_2O_3/Cu-Cr composites are shown in Table 1.

Table 1 Composition of Al_2O_3/Cu-Cr composites

Materials	Al_2O_3 (vol.%)	Cr (vol.%)	Cu (vol.%)
2.8Al_2O_3/Cu	2.8	0	Bal.
2.7Al_2O_3/Cu-0.1Cr	2.7	0.1	Bal.
2.5Al_2O_3/Cu-0.3Cr	2.5	0.3	Bal.
2.3Al_2O_3/Cu-0.5Cr	2.3	0.5	Bal.
2.1Al_2O_3/Cu-0.7Cr	2.1	0.7	Bal.

2.2 Material preparation

The preparation process of Al_2O_3/Cu-Cr composites is shown in Fig. 1, which includes procedures of mixing powders, ball milling, cold isostatic pressing, internal oxidation sintering and reduction, solutioning and hot-extruding, and aging. In the mixing stage, the powders of Cu_2O, Cu-0.6 wt.%Al and Cu-1.5 wt.%Cr were weighed and mixed according to the specified ratio, as seen in Table 1. Then ball milling was carried out in a YXQM-8L planetary ball mill with a ball-to-powder mass ratio of 1:1 for 4 h when the mill ran at a rotating speed of 100 rpm to ensure uniform mixing. The milled powders were placed in a prefabricated rubber sleeve with dimensions of Φ60×150 mm, and were pressed at a pressure of 200 MPa for 5 min using a YLJ-CIP-15 cold isostatic pressing machine. The obtained compacts were sintered in a tube sintering furnace (STG-100-125) in a protective argon atmosphere. The sintering process was performed at a temperature of 1173 K for 6 h to ensure complete oxidation of Al element, followed by 1.5 h of reduction sintering by switching to an atmosphere of hydrogen-argon mixture (Ar-10 vol.%H_2) with a gas

flow rate was 300 rpm to ensure that no Cu_2O was remained. The sintered compacts were solutioning-treated at 1323 K for 1 h, and then subjected to hot extrusion. The hot extrusion was carried out at 1323 K and with an extrusion ratio of 11:1 using a vertical extruder (GYJ-300) to obtain rod-shaped samples of 15 mm in diameter. The extruded samples were finally heat aging-treated at 753 K for 1.5 h in a tube sintering furnace (STG-100-125) protected by an argon atmosphere.

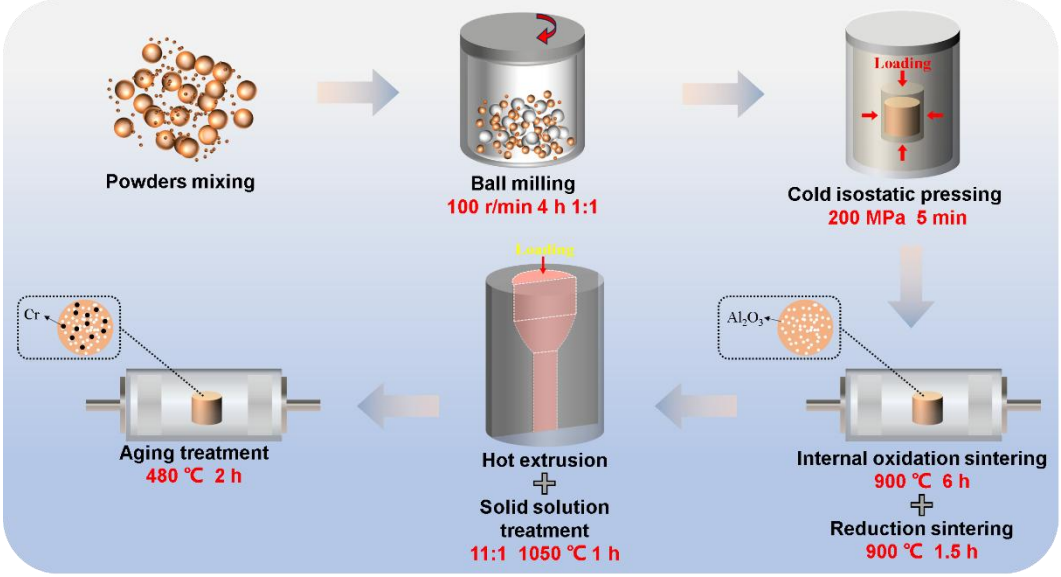

Fig. 1. Schematic diagram of the Al_2O_3/Cu-Cr composites preparation process

2.3 Experimental methods and characterization

The electrical conductivity was measured using a Sigma 2008 B1 Digital Conductivity Meter. The hardness was evaluated using an HBST-3000 digital display Brinell hardness tester with a carbide ball of 5 mm in diameter under a load of 180 kgf and pressure maintaining time of 30 s. The relative density of samples was measured and calculated using a Precisa 321 Precision Balance. To analyze the change in tensile strength of the Al_2O_3/Cu-Cr composites, tensile tests were carried out at room temperature along the extrusion direction using a WDW-100 tensile testing machine at a strain rate of 1 mm/min. The above measurements were taken three times to obtain average values.

The microstructures and element distribution of the composites were characterized using a field emission scanning electron microscope (FE-SEM, JSM-7800 F, JOEL) equipped with energy dispersive spectrometer (EDS). To analyze the strengthening mechanism in detail, electron backscattered diffraction (EBSD) was also performed using the FESEM with an electron backscattering detector. The interfaces between reinforcements and copper matrix were analyzed using a transmission electron microscope (TEM, JSM-2100, JOEL). An X-ray diffractometer (XRD, D8-Advance) was used to characterize the phase composition of composites with Cu Ka radiation and a scanning speed of 0.5°/min. The HRTEM images of reinforcements were analyzed based on the geometric phase analysis (GPA) method, which measures the displacement of atoms in the TEM images below 0.003 nm.

3. Results

3.1 Microstructure of Al_2O_3/Cu-Cr composites

Fig. 2 shows SEM images and EDS 2-dimensional element mapping of the Al_2O_3/Cu-Cr composites with different Cr contents. The elements Al and O are evenly distributed in the copper matrix, suggesting a homogeneous distribution of Al_2O_3 particles in the Al_2O_3/Cu-Cr composites (Fig. 2(a-e)). With the increase in Cr content, the SEM images of $2.3Al_2O_3$/Cu-0.5Cr and $2.1Al_2O_3$/Cu-0.7Cr composites (Fig. 2(d, e)) show black regions, while they are absent in Al_2O_3/Cu-Cr composites with a Cr content below 0.5 vol.% (Fig. 2(b, c)). To further clarify the composition of black regions, elemental analysis is conducted on Al_2O_3/Cu-Cr composites, revealing that the black regions in the $2.3Al_2O_3$/Cu-0.5Cr and $2.1Al_2O_3$/Cu-0.7Cr composites

consist of aggregated Cr particles, whereas the Cr elements in the $2.5Al_2O_3$/Cu-0.3Cr and $2.7Al_2O_3$/Cu-0.1Cr composites exhibit a uniform distribution.

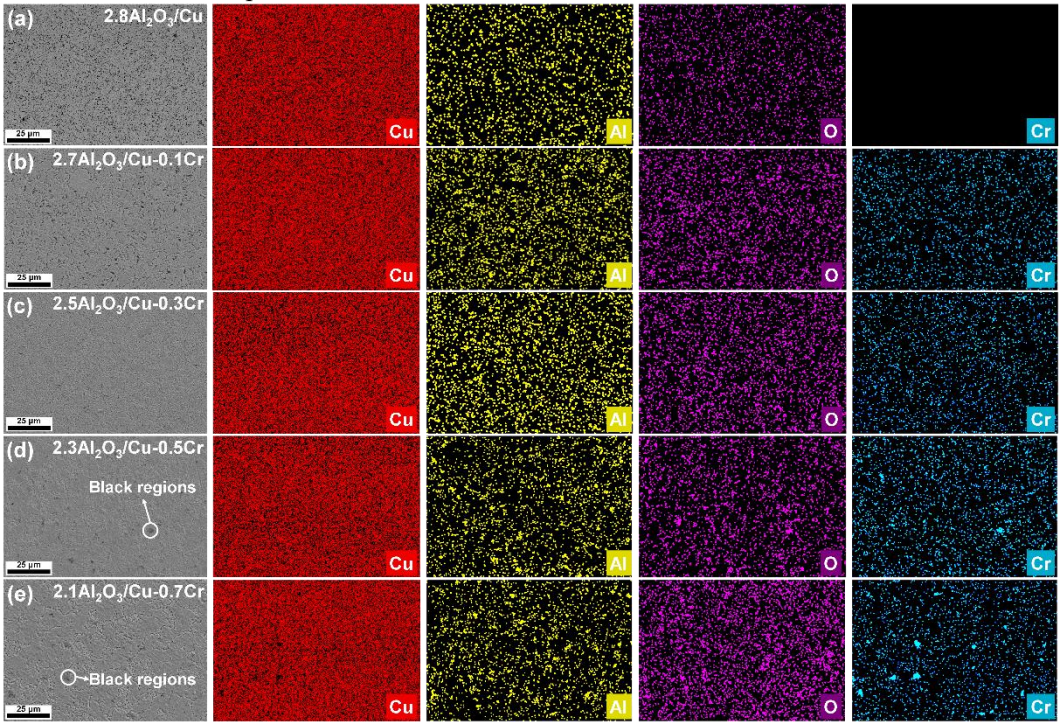

Fig. 2. SEM and EDS images of Al_2O_3/Cu-Cr composites (a) $2.8Al_2O_3$/Cu, (b) $2.7Al_2O_3$/Cu-0.1Cr, (c) $2.5Al_2O_3$/Cu-0.3Cr, (d) $2.3Al_2O_3$/Cu-0.5Cr, (e) $2.1Al_2O_3$/Cu-0.7Cr

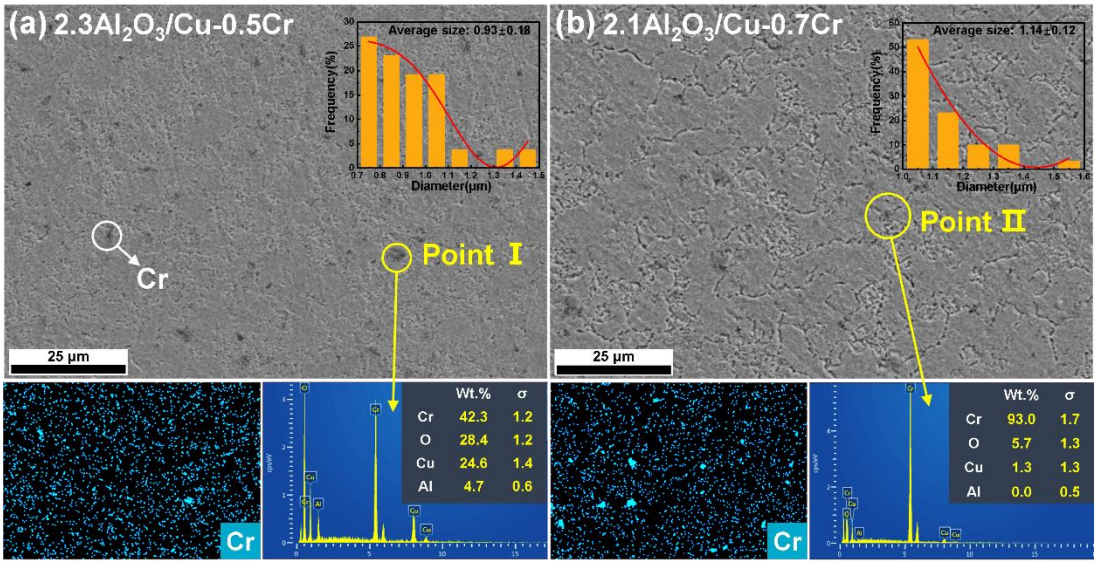

Fig. 3. SEM images and EDS analysis of Al_2O_3/Cu-Cr composites (a) $2.3Al_2O_3$/Cu-0.5Cr, (b) $2.1Al_2O_3$/Cu-0.7Cr

As shown in Fig. 3, the elemental spot scans reveal that the black spots observed in the $2.3Al_2O_3$/Cu-0.5Cr and $2.1Al_2O_3$/Cu-0.7Cr composites correspond to Cr particles with a particle size of approximately 1 μm, whereas the Al_2O_3/Cu-Cr composites with low Cr content exhibit Cr particles sized around 25 nm (Fig. 7 and 8). This suggests that the size of Cr particles changes from nanometer to micrometer with increasing Cr content in the same process, and that the percentage of both changes dynamically. Furthermore, the high error in tensile strength comparison can be attributed to the difficulty in counting the proportion of nano and micro-Cr particles. It can be inferred that Orowan strengthening by nano-Cr particles will be weakened due to particle aggregation, while micro-Cr particles will play a role in load transfer strengthening for Al_2O_3/Cu-Cr composites. This finding implies that different heat treatment processes can

effectively regulate the size and distribution of Cr particles of Al_2O_3/Cu-Cr composites. Consequently, achieving precise control over the nanoscale dimensions of Cr particles becomes a crucial objective for optimizing the manufacturing process.

Fig. 4 shows XRD curves of the Al_2O_3/Cu-Cr composites with different Cr content. The curves contain only diffraction peaks of the Cu matrix whereas other possible phases, such as Al_2O_3, were not detected. The intensity of the $(111)_{Cu}$ diffraction peak gradually decreases with the increase of Cr content, while the intensity of the $(200)_{Cu}$ diffraction peak gradually increases. Some studies [22-24]reported that the $\{111\}_{Cu}$ and $\{110\}_{Cu}$ hard orientation decreased with increasing heat treatment temperature, which favored the formation of $\{001\}_{Cu}$ soft orientation. The grain growth of $\{001\}_{Cu}$ was attributed to the easy migration of its own grain boundaries. This may provide an explanation to the grain growth and change in orientation of the Al_2O_3/Cu-Cr composites in this work. For Al_2O_3/Cu-Cr composites, the softening resistance of Al_2O_3/Cu-Cr were weakened by the reduction of Al_2O_3 nanoparticle content. The incorporation of Cr could reduce the interfacial stress of Al_2O_3/Cu-Cr composites, making dislocations and grain boundaries easier to migrate. Therefore, the Al_2O_3/Cu-Cr composites underwent changes in grain orientation and size with the change of Cr content at the same heat treatment temperature.

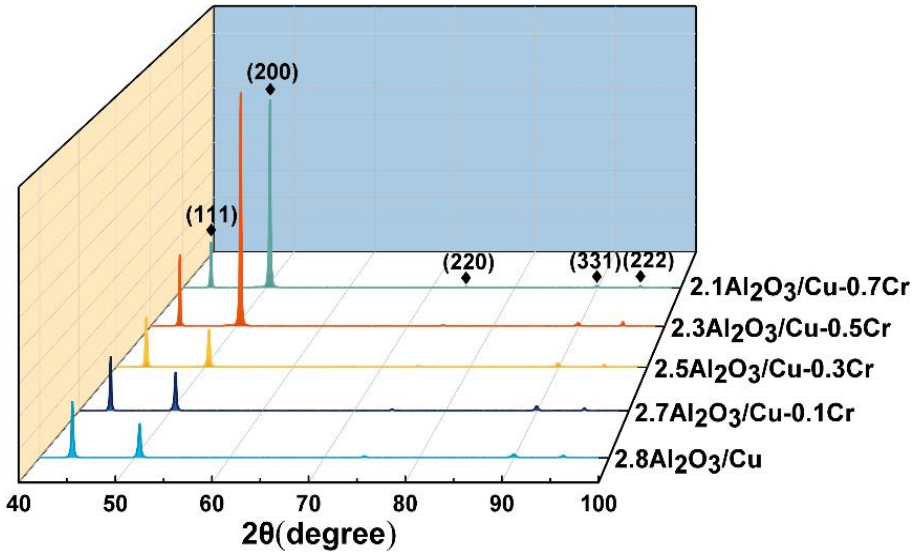

Fig. 4. XRD curves of Al_2O_3/Cu-Cr composites

The obtained XRD curves also allowed precise determination of the lattice parameter of the Cu matrix. Fig. 5 shows the effects of Cr incorporation and heat treatments on the lattice parameter. The $2.8Al_2O_3$/Cu sample shows a lattice constant of 3.61717 Å. Incorporation of Cr led to increased lattice constant, e.g., 3.61766 Å for the $2.5Al_2O_3$/Cu-0.3Cr and 3.61827 Å for the $2.1Al_2O_3$/Cu-0.7Cr. The maximum lattice expansion was obtained in the $2.1Al_2O_3$/Cu-0.7Cr when the Cr content approached the solid solubility (0.81 vol.%) of Cr in a Cu matrix [25]. After aging treatment, the lattice constants of the Al_2O_3/Cu-Cr composites gradually lowered to the same level as those of the $2.8Al_2O_3$/Cu composites, indicating precipitation of Cr particles from the Cu matrix. The results imply that Cr particles might have agglomerated during the aging process regardless of the amount of Cr incorporation. Like most elemental precipitation processes, preferential nucleation sites such as grain boundaries, dislocations, and second phases should have played a role in facilitating the Cr precipitation. Previous research by Sheibani et al. [26-28] found that high density dislocations and tissue defects caused by Al_2O_3 incorporation promoted effective diffusivity of Cr and accelerated its aging precipitation response.

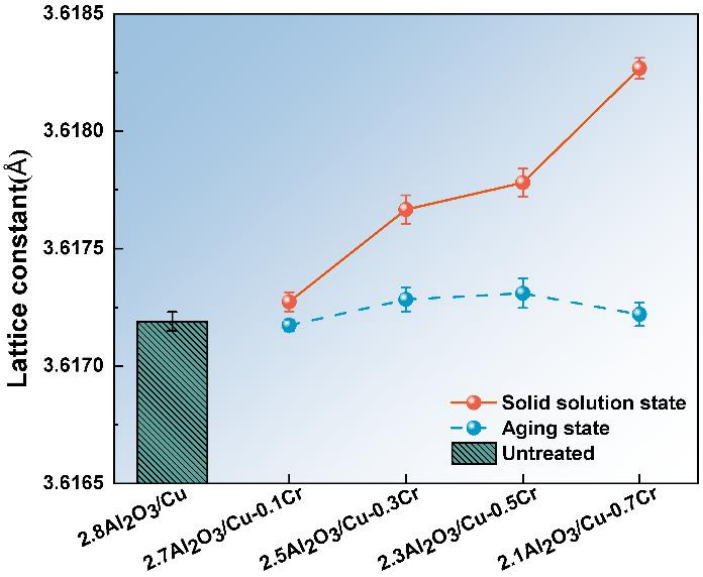

Fig. 5. Effect of heat treatment on the lattice constants of Al_2O_3/Cu-Cr composites

Fig. 6(a-e) shows SEM-EBSD analyses of the Al_2O_3/Cu-Cr composites, including inverse pole figures (IPF) and the grain size statistics. The EBSD diagram represents the cross-section of the material. With increasing Cr content, the IPF images show that the grains break under the applied load, and the Al_2O_3/Cu-Cr composites exhibit a decrease in the proportion of $[111]_{Cu}$ (blue grains), while the proportion of $[001]_{Cu}$ (red grains) gradually increases with increasing Cr content. In general, a progressive increase in the grain size with increasing Cr content can be observed. This variation is featured both by the increased average grain size and by the decreased number of grains. Meanwhile, the grain size statistics also indicate a gradual increase in the grain size deviation, e.g., from 0.94 μm of the $2.8Al_2O_3$/Cu and 2.54 μm in the $2.1Al_2O_3$/Cu-0.7Cr. The grain coarsening might be closely associated with the softening of the material. Fig. 6(f) shows a classification of the imaged granular microstructure that each sample comprised three types of grains, namely, the deformed, sub-structured and recrystallized grains. The Cr-containing composites contained more recrystallized and sub-structured grains than the Cr-free composite, indicating contribution of the Cr incorporation to the recrystallisation kinetics. These results indicate that the microstructure of the material underwent softening during the heat treatment.

It is worth mentioning that the volume fraction of recrystallized grains of Al_2O_3/Cu-Cr composites show an increasing trend with the increase of Cr content. Previous research by Savaedi et al. [29] has shown that dynamic recrystallization occurs when the hot activation energy of a material reaches a critical threshold for this process. The study by Zhang et al.'s [30] on the high-temperature fracture stability of Cu, CuCrZr and Cu-Al_2O_3 materials revealed that nano-Al_2O_3 particles could significantly inhibit the occurrence of dynamic recrystallization due to the hindering effect of nano-Al_2O_3 particles on the migration of grain boundaries and dislocation movement, which hindered the process of substructural transformation and grain growth. Thus, the reduction of Al_2O_3 content and the agglomeration of Cr particles weaken the inhibitory effect of nanoparticles on dynamic recrystallization, and thus enhance the softening behavior of Al_2O_3/Cu-Cr composites.

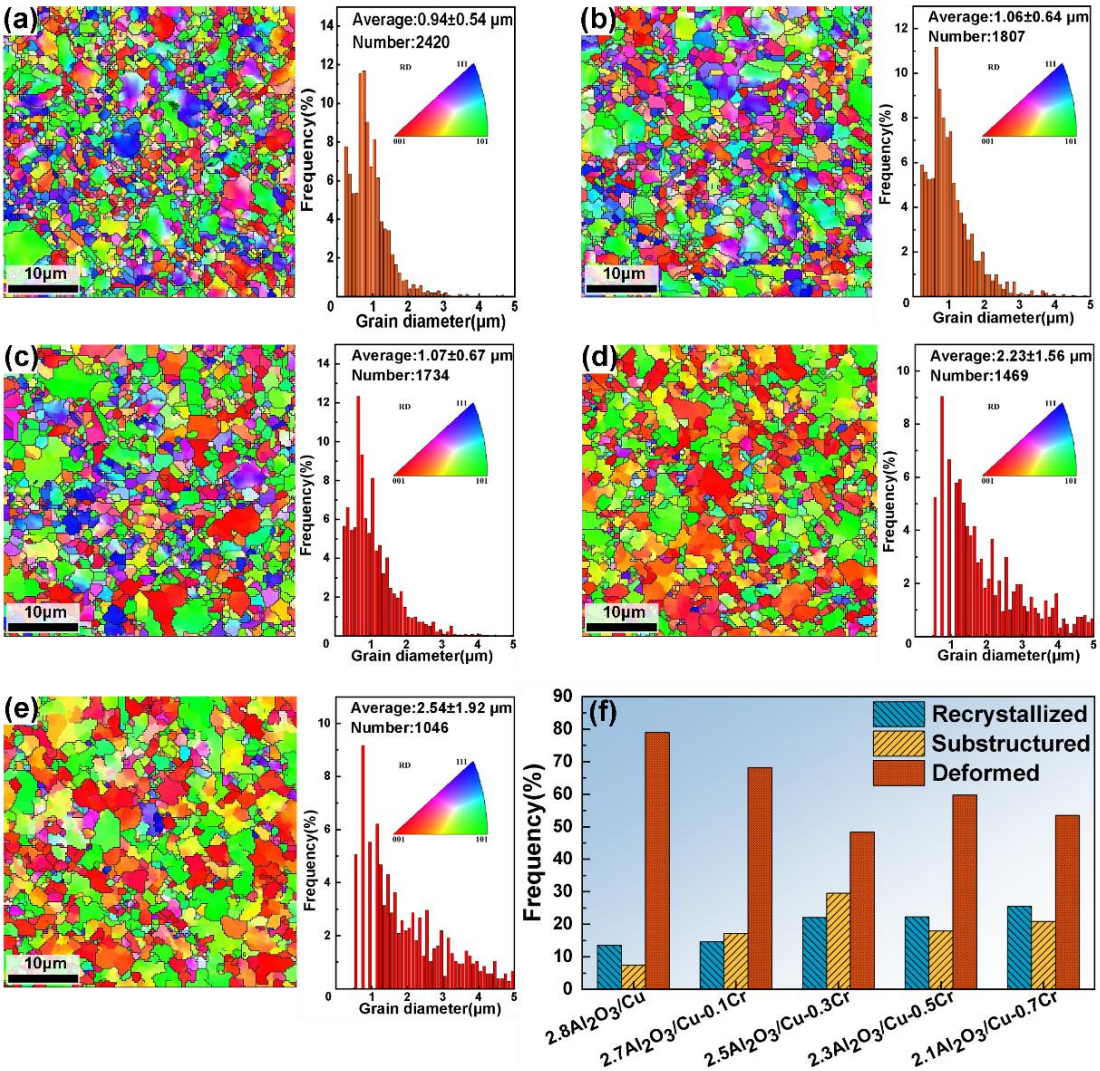

Fig. 6. IPF images of Al_2O_3/Cu-Cr composites (a) 2.8Al_2O_3/Cu, (b) 2.7Al_2O_3/Cu-0.1Cr, (c) 2.5Al_2O_3/Cu-0.3Cr, (d) 2.3Al_2O_3/Cu-0.5Cr, (e) 2.1Al_2O_3/Cu-0.7Cr, (f) Grain frequency statistics

TEM analyses were conducted to reveal the structural characteristics of Al_2O_3 and Cr particles in the $2.5Al_2O_3$/Cu-0.3Cr composite. Fig. 7a is a bright field TEM image showing uniform dispersion of Al_2O_3 particles in the Cu matrix. Fig. 7b is a zero-loss image at a higher magnification showing the size and shape of two Al_2O_3 particles, whereas Fig 8c is a fast Fourier transform (FFT) pattern confirming the presence of γ-Al_2O_3 crystalline structure. The Al_2O_3 particles in Figs 7a and 7b exhibit an average size of approximately 8 nm. Fig. 7d is a high-resolution TEM (HRTEM) image of the Cu/Al_2O_3 interface, from which the interface mismatch was calculated to be 8.89%. Figs. 8 a-d show similar analyses of the Cr particles in the Cu matrix. The Cr particles exhibit an average diameter of 25 nm, whereas the Cr/Cu interface shows a small mismatch of 6.67%.

It is known that the reinforcing phase is completely coherent with the matrix if the mismatch is less than 5% or completely incoherent if the mismatch exceeds 25%. In this work, both the Al_2O_3-Cu and Cr-Cu interfacial mismatches are far less than 25%, suggesting that the nano-Al_2O_3 and Cr particles form semi-coherent interfaces with the Cu matrix. Such semi-coherent interfaces are more favorable for enhancing deformation stability than incoherent interfaces.

The effective inhibition of nanoparticles on dislocations plays a crucial role in maintaining the high mechanical properties of Al_2O_3/Cu-Cr composites, indicating a synergistic enhancement effect between Al_2O_3 and Cr. For synergistically reinforced copper matrix composites, diffusely distributed reinforcements and a good interfacial relationship are maximized to improve the performance of copper composites [31].

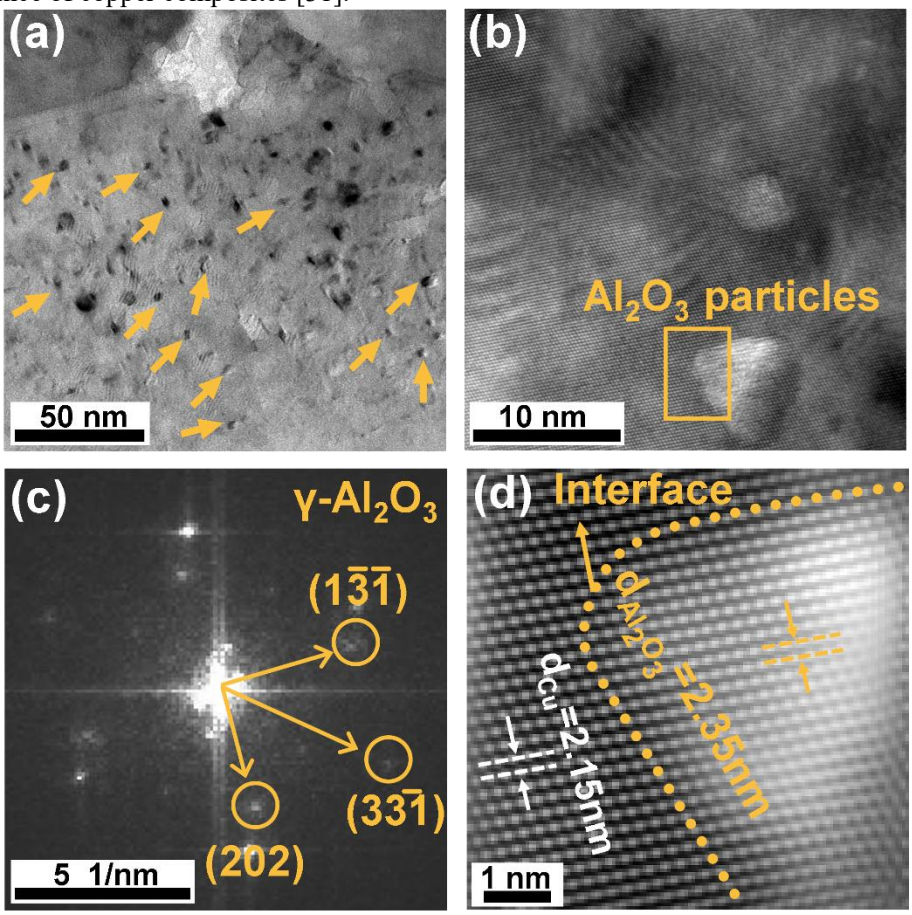

Fig. 7. TEM analyses of Al_2O_3 nanoparticles in the $2.5Al_2O_3$/Cu-0.3Cr composite: (a) A BF image showing Al_2O_3 particles on Cu matrix; (b) A defocused zero-loss image showing two Al_2O_3 particles; (c) A FFT pattern of the Al_2O_3 particles; and (d) A HRTEM image of the Al_2O_3-Cu interface.

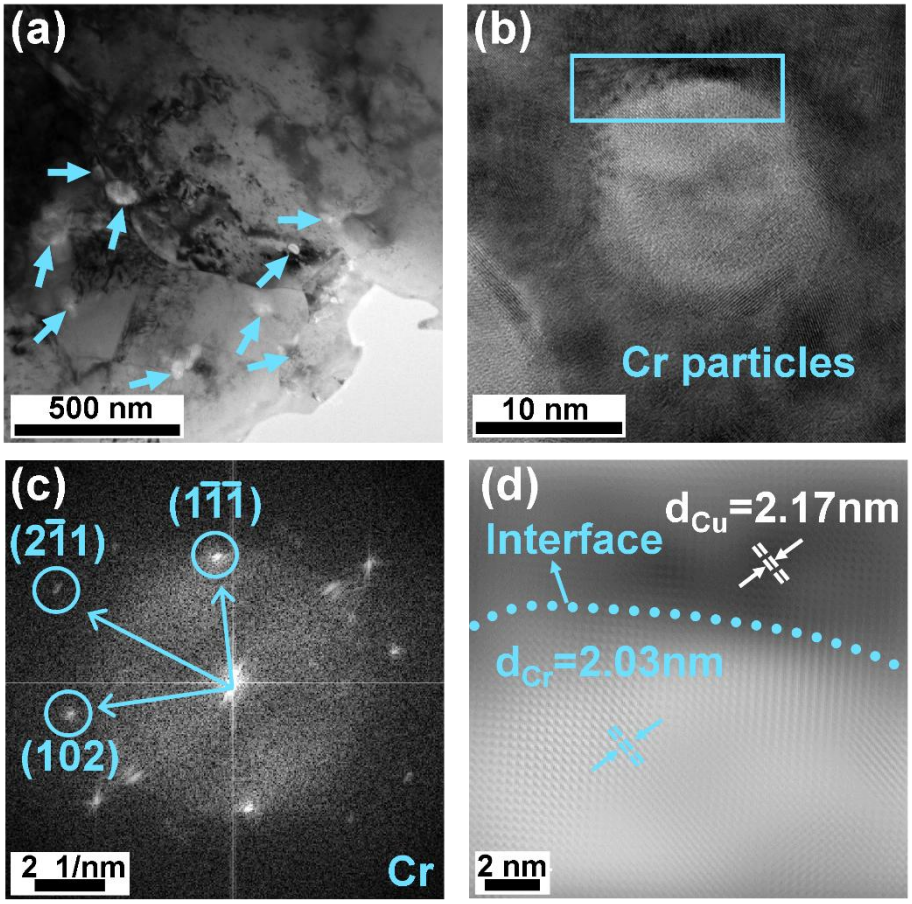

Fig. 8. TEM analyses of Cr nanoparticles in the 2.5Al_2O_3/Cu-0.3Cr composite: (a) A BF image showing Cr particles in Cu matrix; (b) A defocused zero-loss image showing a Cr particle; (c) A FFT pattern of the Cr particles; and (d) A HRTEM image of the Cr-Cu interface.

Figs. 9a and 9d show HRTEM images of an Al_2O_3 particle and a Cr particle, respectively. Figs. 9b and 9c display the microscopic strain distributions in the same imaged area along the longitudinal (X) and transverse (Y) directions respectively. Among them, longitudinal X represents the extrusion direction and transverse Y represents the vertical extrusion direction. Different colors indicate different strain variables, with positive values indicating tensile strain and negative values indicating compressive strain. A significant transition in strain value along the Al_2O_3-Cu interface was observed in the X direction accompanied by a change in direction. However, there is no significant difference in strain value in the transverse direction. These indicate that tensile strain dominates around Al_2O_3 particles due to longitudinal tension and transverse compression driven by applied loads.

Figs. 9e and 9f display the strain fields along the X and Y direction respectively. Unlike the Al_2O_3-Cu interface, the Cr-Cu interface exhibited fluctuating strain values both in the longitudinal and transverse directions, suggesting alternate atom displacement under tensile and compressive stresses. The different strain fields between the two types of interfaces imply that different responses of the Al_2O_3 and Cr particles to the deformation. A deformation discordance existed between the Al_2O_3 particles and the Cu matrix in deforming of Al_2O_3/Cu-Cr composites, whereas a better synergistic deformation was achieved between the Cr particles and Cu matrix. In literature, Wang et al. [32] simulated the interface of Cu-1 wt.%Cr-4 wt.%Al_2O_3 composites and found that the interfacial residual stress of Cu/Al_2O_3 (39.4 MPa) was higher than that of the Cu/Cr interface (7.67 MPa). This is in good consistence to the findings of current research that the Al_2O_3 particles had a higher deformation resistance than the Cr particles in the deformation process.

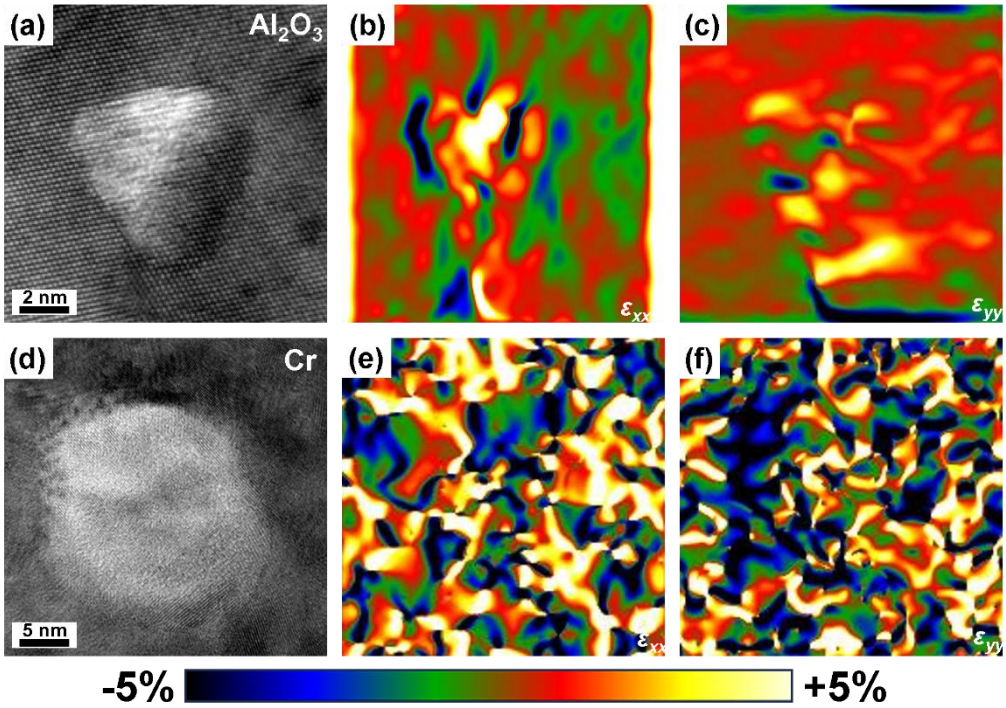

Fig. 9. GPA analysis of 2.5Al_2O_3/Cu-0.3Cr composite (a) Al_2O_3 particle, (b) Strain field image of Al_2O_3 particle in X direction, (c) Strain field image of Al_2O_3 particle in Y direction, (d) Cr particle, (e) Strain field image of Cr particle in X direction, (f) Strain field image of Cr particle in Y direction

3.2 Physical properties of Al_2O_3/Cu-Cr composites

Fig. 10 shows the influence of Cr incorporation on the electrical conductivity and mechanical properties of the Al_2O_3/Cu-Cr composites. The data are summarized in Table 2. Typical engineering stress-strain curves are shown in Fig. 11. In Fig. 10a, the electrical conductivity of the fabricated composites falls in a range of 75 ~ 81, accounting for 76-81% of the conductivity of pure copper. Incorporation of Cr led to a slight increase of the conductivity as compared to the Cr-free composite. This can be attributed to the insulating nature of Al_2O_3 particles, and the superior conductivity of Cr particles compared to Al_2O_3 particles. As the Cr content increases, there is a gradual weakening in electron scattering by reinforcement particles, resulting in an incremental enhancement in electrical conductivity for the Al_2O_3/Cu-Cr composites. Furthermore, during internal oxidation process impurity elements present in Cu undergo oxidation which contributes to restoring electrical conductivity [33].

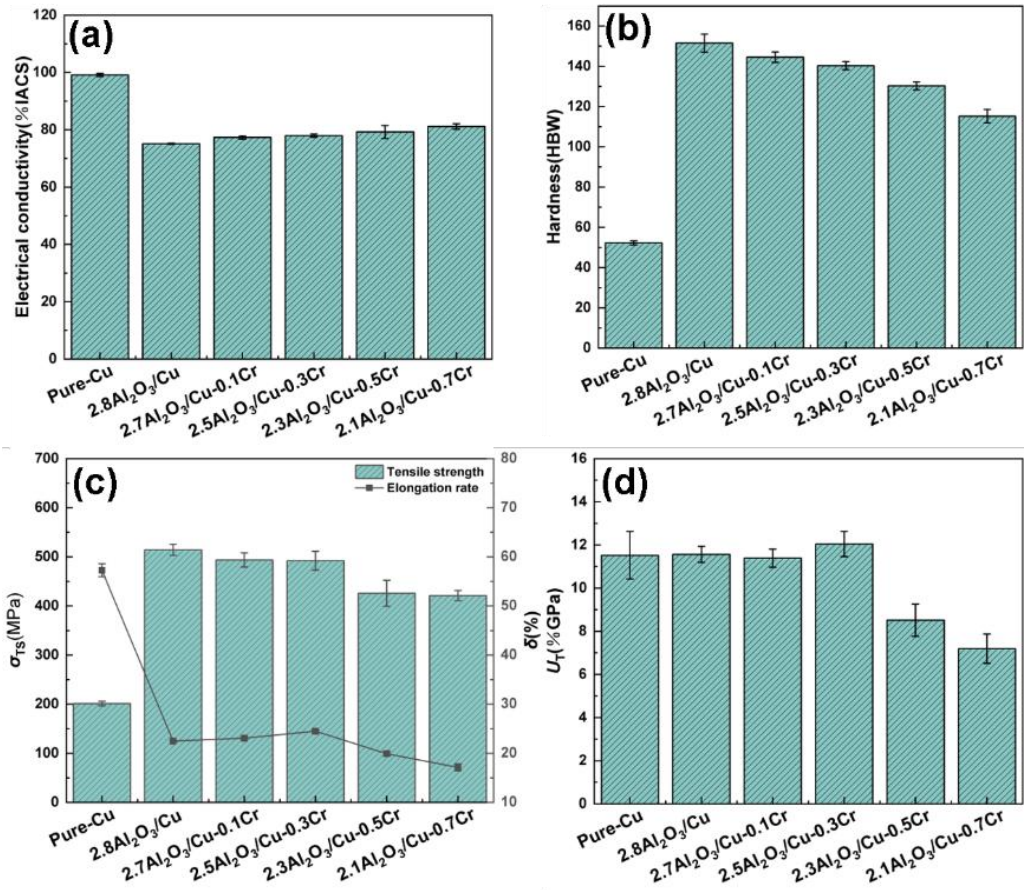

Fig. 10. Changes in physical properties of Al_2O_3/Cu-Cr composites (a) Electrical conductivity, (b) Hardness, (c) Tensile strength and Elongation rate, (d) U_T

Fig. 11 shows the engineering stress-strain curves of Al_2O_3/Cu composites determined at room temperature. In the tensile tests, both the pure copper and the copper matrix composites underwent elastic deformation, yield, plastic deformation and necking fracture stages. The plastic deformation stage significantly affected the elongation change of the composites [6]. The variations of the hardness and ultimate tensile strength show a trend that the Cr-free composite possesses the highest hardness and strength, as shown in Figs. 10b and 10c. Incorporation of Cr in the composites resulted in a decrease of the properties, which however is less than 10% in the composites containing 0.1% and 0.3% of Cr. On the other hand, the composites containing 0.1% and 0.3% of Cr showed a significant increase in the elongation property, namely, 2.02% higher than the Cr-free composite, as shown in Fig. 10c. Consequently, the best toughness property was obtained in the composites containing 0.3% Cr, i.e., 0.48% higher than the Cr-free composite.

Table 2 Physical properties of Al_2O_3/Cu-Cr composites

Materials	Relative density (%)	Electrical conductivity (%IACS)	Hardness (HBW)	σ_{TS} (MPa)	δ (%)	U_T (GPa%)
Cu [34]	99.9	99.13 (±0.53)	52.24 (±1.04)	201.22 (±4.81)	57.27 (±1.34)	11.52 (±1.10)
2.8Al_2O_3/Cu	97.5	75.14 (±0.21)	151.52 (±4.43)	514.23 (±11.24)	22.47 (±0.22)	11.56 (±0.37)
2.7Al_2O_3/Cu-0.1Cr	97.4	77.35 (±0.57)	144.55 (±2.57)	493.58 (±14.43)	23.06 (±0.17)	11.39 (±0.42)
2.5Al_2O_3/Cu-0.3Cr	97.4	77.96 (±0.53)	140.31 (±2.04)	492.07 (±19.04)	24.48 (±0.24)	12.04 (±0.58)
2.3Al_2O_3/Cu-0.5Cr	97.4	79.23 (±2.26)	130.27 (±1.97)	425.76 (±26.42)	19.92 (±0.53)	8.51 (±0.75)
2.1Al_2O_3/Cu-0.7Cr	97.4	81.16 (±0.94)	115.24 (±3.35)	421.04 (±10.11)	17.14 (±0.71)	7.19 (±0.68)

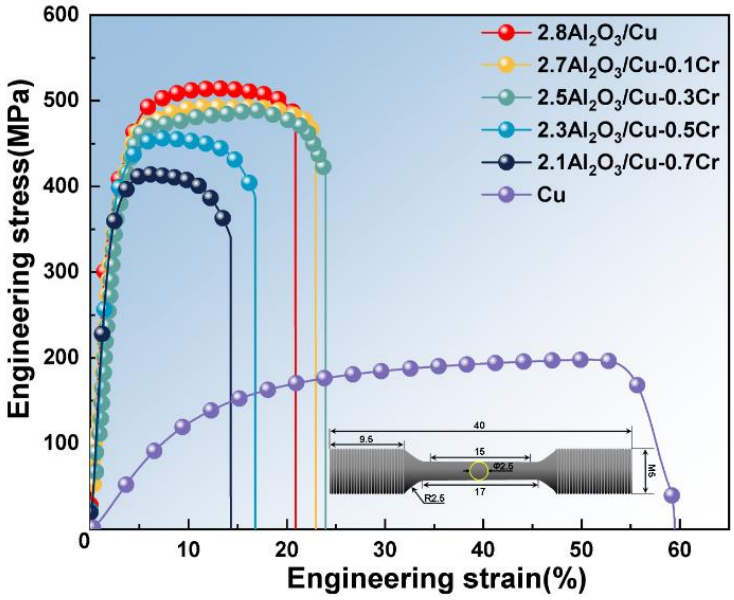

Fig. 11. Engineering stress-strain curves of Al_2O_3/Cu-Cr composites

The hindering effect of Cr particles on dislocations is weaker compared to that of Al_2O_3 particles due to the differences in sizes, distribution states, and contents between the two, leading to a weaker promotion of strength by increasing Cr particles content than the reduction of strength by decreasing Al_2O_3 particles content. Therefore, the tensile strength of Al_2O_3/Cu-Cr composites tend to decrease with the increase of Cr content. For the change of Al_2O_3/Cu-Cr composites elongation, the percentage of Al_2O_3 and Cu interface in Al_2O_3/Cu-Cr composites decrease with the increase of Cr content, while the percentage of Cr and Cu interface increases. Moreover, because the σ_{Cu/Al_2O_3} is lower than that of $\sigma_{Cu/Cr}$ and there is an incongruous deformation between the Al_2O_3 particles and the Cu matrix, which will help Cr to improve the elongation of Al_2O_3/Cu-Cr composites (Fig. 7 and 8). Furthermore, heat treatment facilitates a transformation from $[111]_{Cu}$ hard orientation to $[100]_{Cu}$ soft orientation, which further promotes elongation properties of Al_2O_3/Cu-Cr composites (Fig. 6).

It is noteworthy that the elongation behavior of Al_2O_3/Cu-Cr composites exhibit an initial increase followed by a significant decrease. In a study conducted by Duan et al. [35], it was observed that the aggregated Cr particles in precipitated WC/CuCr30 composites were elongated along the extrusion direction during the extrusion process, which resulted in cracks within the Cr particles. Similarly, Shen et al. [36] reported that deformation of a Cu-15Ni-8Sn alloy with precipitated γ phase resulted in crack formation and subsequent material fracture due to crack propagation. In current research, the Al_2O_3 particles acted as favorable nucleation sites for Cr precipitation, thereby reducing the activation energy required for Cr precipitation. Thus, the aggregation of Cr particles may be related to the reduction of elongation of Al_2O_3/Cu-Cr composites.

Fig. 12 shows a schematic diagram of the fracture failure process of Al_2O_3/Cu-Cr composites caused by the aggregation of Cr particles. When the load was not applied, the Cr particles were still in the state after aging treatment. As the load gradually increased, the aggregated Cr particles were elongated along the tensile direction, which tended to induce microcracks in the Cr particles. With further increase in load, there was a high likelihood of cracking occurring at the Cu/Al_2O_3 interface due to elevated internal stress around the Al_2O_3 particles. Ultimately, this led to material fracture as cracks propagate and establish interconnections with voids and other cracks.

There was an equilibrium point between tensile strength and elongation of Al_2O_3/Cu-Cr composites with the variation of reinforcements content. The product of tensile strength and elongation (U_T) of material comprehensively considers the correlation between strength and plasticity[37-38]. A greater value of U_T indicates that the material absorbs more energy per-unit volume during deformation, which makes the material deformation more stable. The U_T values of Al_2O_3/Cu-Cr composites with different Cr contents can be obtained by calculating Eq. 2 [39], and the results are listed in Table 2. The 2.5Al_2O_3/Cu-0.3Cr composite has a maximum U_T value of 15.8 GPa%, it shows that the 2.5Al_2O_3/Cu-0.3Cr composites have the optimal mechanical

properties.

$$U_T = \sigma_{TS} \cdot \delta \quad (1)$$

where σ_{TS} and δ are the tensile strength and elongation of Al_2O_3/Cu-Cr composites, respectively.

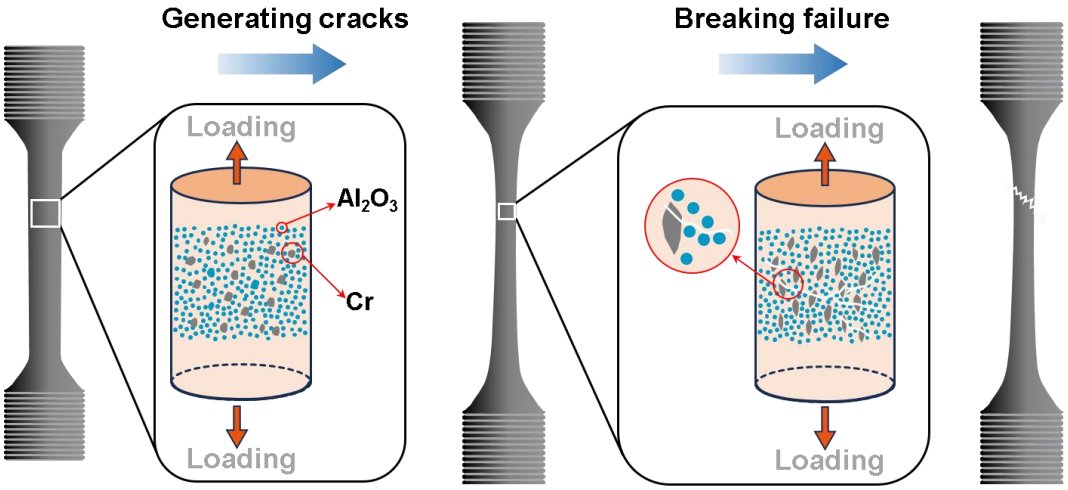

Fig. 12. Schematic diagram of fracture induced by Cr particle aggregation in Al_2O_3/Cu-Cr composites

4. Discussion

The change in the content of reinforcements resulted in different strengthening effects for the Al_2O_3/Cu-Cr composites. In general, grain refining, solid solution strengthening, dislocation strengthening, precipitation strengthening and Orowan strengthening are mainly considered for tensile strength of metallic materials [40-41]. The present study mainly considers grain strengthening, dislocation strengthening, Orowan strengthening induced by nano-Al_2O_3 and Cr particles. The grain strengthening can be calculated by the Hall-Patch equation (Eq. 3) [42]:

$$\Delta\sigma_{GR} = K(d_c^{-0.5} - d_m^{-0.5}) \quad (2)$$

where K is a constant (0.07 MPa · $m^{0.5}$ for Cu), d_c and d_m are the average sizes of the composites and pure Cu.

The dislocation density of Al_2O_3/Cu-Cr composites is significantly changed due to the hot extrusion and heat treatment, while the dislocation strengthening can be calculated by Taylor's equation (Eq. 4) [43]:

$$\Delta\sigma_{DIS} = M\alpha Gb\sqrt{\rho} \quad (3)$$

where M is the Taylor factor for copper with a value of 3.06, α is the strength coefficient of the dislocation of copper (0.2), G is the shear modulus (47.7 GPa), b is the Burgers vector (0.256 nm) of copper, and ρ is the dislocation density of the Al_2O_3/Cu composites.

The nano-Al_2O_3 and Cr particles were formed by internal oxidation combined with heat treatment methods, while the strengthening effect induced by the nanoparticles can be calculated using Orowan's equation (Eq. 5 and Eq. 6) [43]. In this study, it is assumed that the Al_2O_3/Cu-Cr composites have the similar size of the reinforcements under the identical process.

$$L = r\left(\sqrt{\frac{\pi}{6f}} - \frac{\pi}{4}\right) \quad (4)$$

$$\Delta\sigma_{OR} = \frac{0.4Gb}{\pi\sqrt{1-\nu}} \cdot \frac{1}{L} \cdot \ln\left(\frac{r}{b}\right) \quad (5)$$

In Eq. 4 and Eq. 5, r is the average radius of reinforcement particles, v is the Poisson's ratio of copper, which is taken as 0.35, f is the volume fraction of reinforcement particles.

The tensile strengths of Al_2O_3/Cu-Cr composites with different contents can be obtained by Eq. 7, where σ_m is the tensile strength of the copper matrix[44-45].

$$\sigma_{TS} = \sigma_m + \Delta\sigma_{GR} + \Delta\sigma_{DIS} + \Delta\sigma_{OR}^{Al_2O_3} + \Delta\sigma_{OR}^{Cr} \quad (6)$$

The calculated strengthening contributions are listed in Table 3. As seen, the value of Orowan strengthening induced by Cr particles gradually increases due to the increase in Cr content, while

the value of Orowan strengthening caused by Al_2O_3 particles gradually decreases. Furthermore, the contribution values of grain and dislocation strengthening of Al_2O_3/Cu-Cr composites are changed due to the alteration of grain size and dislocation density. Additionally, an assessment of experimental and calculated values reveals an error exceeding 10% for both 2.3Al_2O_3/Cu-0.5Cr and 2.1Al_2O_3/Cu-0.7Cr composites.

Table 3 Calculated strengthening contributions of Al_2O_3/Cu-Cr composites

Materials	d (μm)	ρ ($10^{13}\cdot m^{-2}$)	$\Delta\sigma_{GR}$ (MPa)	$\Delta\sigma_{DIS}$ (MPa)	$\Delta\sigma_{OR}^{Al_2O_3}$ (MPa)	$\Delta\sigma_{OR}^{Cr}$ (MPa)	σ_{Error} (%)
2.8Al_2O_3/Cu	0.94	4.02	59.90	47.37	203.20	-	0.54
2.7Al_2O_3/Cu-0.1Cr	1.06	3.46	55.90	43.99	198.75	13.86	3.89
2.5Al_2O_3/Cu-0.3Cr	1.07	2.71	55.54	38.89	189.70	24.65	3.49
2.3Al_2O_3/Cu-0.5Cr	2.23	1.43	34.72	28.25	180.43	32.42	10.73
2.1Al_2O_3/Cu-0.7Cr	2.53	2.00	31.84	33.39	170.91	38.95	11.58

Fig. 13(a) shows the contribution statistics of different strengthening mechanisms in Al_2O_3/Cu-Cr composites. The results show that the tensile strength of Al_2O_3/Cu-Cr composites is mainly dominated by matrix strengthening and the Orowan strengthening induced by Al_2O_3 particles, while grain strengthening, dislocation strengthening, and the Orowan strengthening induced by Cr particles play a secondary role. It is noteworthy that the contribution of Orowan strengthening induced by Cr particles increases from 0% to 8% with the change of Cr content, while the grain strengthening decreases from 12% to 7%. It is attributed to the fact that the increase in Cr nanoparticle content promotes the hindering effect of nanoparticles on the dislocation movement, which results in a significant increase in the Orowan strengthening induced by Cr particles. Meanwhile, the improvement of interfacial stress by Cr particles and the weakening of the softening resistance of Al_2O_3/Cu-Cr composites result in a gradual increase of grain size with the increase of Cr content, which in effect weakens the contribution of grain strengthening to the tensile strength of Al_2O_3/Cu-Cr composites. In addition, the contribution of dislocation strengthening is less variable, and the large proportion of Orowan strengthening by Al_2O_3 particles and matrix strengthening make the contribution of the three types of strengthening fluctuate less. From the theoretical calculations, it can be seen that the introduced Cr particles improve the interfacial relationship and the degree of softening of Al_2O_3/Cu composites, which leads to the change of grain size and dislocation density of Al_2O_3/Cu-Cr composites, and the change of the Cr content changes the degree of contribution of Orowan strengthening, which leads to the tensile strength of Al_2O_3/Cu-Cr composites was made to decrease with the increase of Cr content.

Fig. 13(b) shows a linear fitting relationship between the experimental and calculated values of tensile strength of Al_2O_3/Cu-Cr composites, and its result shows that the correlation coefficient R^2 is 0.95, which validates the calculation validity of the strength contribution of Al_2O_3/Cu-Cr composites based on the mechanism of grain strengthening, dislocation strengthening and Orowan strengthening.

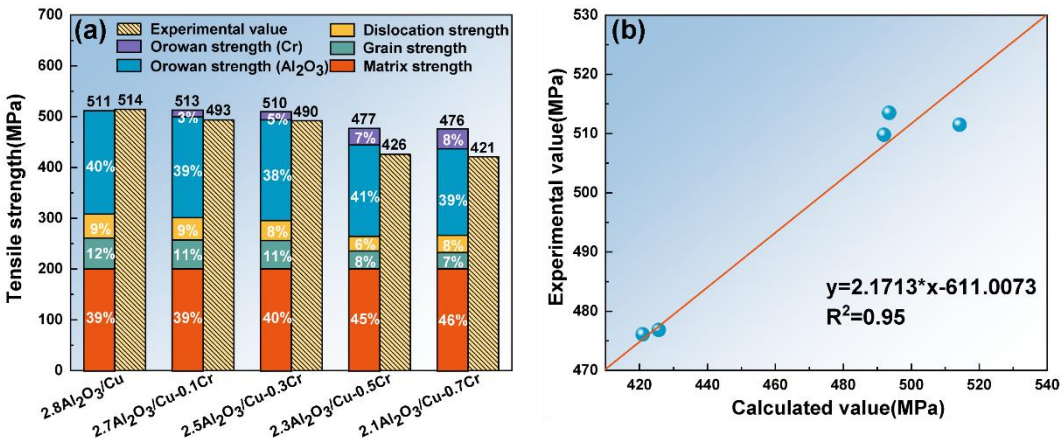

Fig. 13. Contribution statistics of different strengthening mechanisms in Al_2O_3/Cu-Cr composites (a) proportion of strengthening contribution, (b) correlation of experimental and calculated values

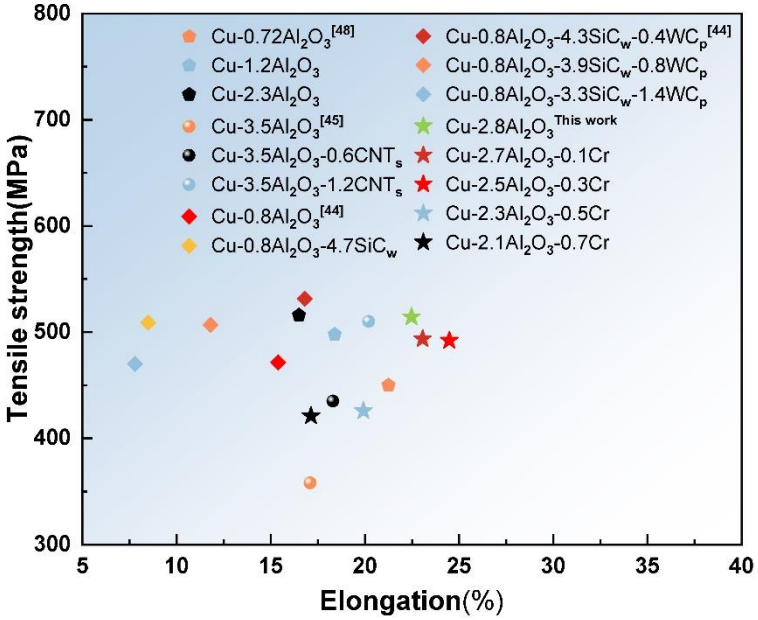

Fig. 14. Comparison of strength and elongation of Al_2O_3/Cu composites

Fig. 14 shows a comparison of the matching relationship between strength and elongation of Al_2O_3/Cu composites prepared by internal oxidation method. It can be seen that the changes of strength and elongation of Al_2O_3/Cu composites are closely related to the content of Al_2O_3 in their materials. Just as J. Lee et al. [46] prepared Al_2O_3/Cu composites under the same process, whose results found that the strength of Al_2O_3/Cu composites increased with the increase of Al_2O_3 content, but the elongation gradually decreased. This indicated that the Al_2O_3 content plays a key role in the mechanical properties of Al_2O_3/Cu composites. F. Long et al. [43] prepared Al_2O_3/Cu-CNT_s composites with different CNT_s contents, and their results found that the elongation and mechanical properties of Al_2O_3/Cu-CNT_s showed an upward trend with the increase of CNT_s content. H.R. Lin et al. [42] also improved the strength and elongation of Cu-0.8vol.%Al_2O_3/Cu composites by synergistic adjustment of SiC_w and WC_p. Compared to the results of previous studies, the present study improved the plastic deformability of Al_2O_3/Cu-Cr composites through the synergistic adjustment of Al_2O_3 and Cr. The optimal balance of strength and elongation of Al_2O_3/Cu-Cr composites were realized on the basis of ensuring the strength of Al_2O_3/Cu composites.

5 Conclusion

In this paper, Al_2O_3/Cu-Cr composites with different Cr contents were fabricated by internal oxidation and heat treatment methods. The effect of Cr content on the microstructure and plastic deformability of Al_2O_3/Cu-Cr composites was investigated, the microstructure of synergistic improvement of plastic deformability of copper matrix composites by Al_2O_3 and Cr was revealed, and the strengthening mechanisms of A_2O_3/Cu-Cr composites were analyzed in detail. The main conclusions are as follows:

(1) The A_2O_3/Cu-Cr composites showed a microstructure comprising Cu matrix and uniformly dispersed nano-particles of Al_2O_3 and Cr. The nano-Al_2O_3 and Cr particles both have semi-coherent interfaces with the Cu matrix. The Al_2O_3/Cu-Cr composite underwent a transition from the hard $[111]_{Cu}$ orientation to the soft $[100]_{Cu}$ orientation with increasing Cr content, resulting in different degrees of dynamic recrystallization of the Al_2O_3/Cu-Cr composites. The Al_2O_3 particles demonstrated a distinct deformation discrepancy with the Cu matrix, whereas a more favorable synergistic deformation was achieved between the Cr particles and Cu matrix, thereby significantly enhancing the plastic deformability of Al_2O_3/Cu-Cr composites.

(2) The electrical conductivity and hardness of the Al_2O_3/Cu-Cr composites showed a decreasing trend with increasing Cr content. The elongation of 2.5Al_2O_3/Cu-0.3Cr

composite increased to 24.48% from 22.47% of the Cr-free 2.8Al_2O_3/Cu composite, while the tensile strength showed a marginal decrease to 492 MPa as compared to 514 MPa of the 2.8Al_2O_3/Cu composite.

(3) The tensile strength of Al_2O_3/Cu-Cr composites was mainly dominated by matrix strengthening and the Orowan strengthening induced by Al_2O_3 particles, while grain strengthening, dislocation strengthening, and the Orowan strengthening induced by Cr particles play a secondary role. The correlation coefficient R^2 was 0.95 after fitting the experimental and calculated values of tensile strength.

Data availability

The authors do not have permission to share data.

CRediT authorship contribution statement

Xiuhua Guo: Data curation, Investigation, Methodology, Writing -original draft. **Guoyang Xu**: Conceptualization, Investigation, Writing original draft. **Shaolin Li**: Writing review, Funding acquisition. **Kexing Song**: Writing − review & editing, Funding acquisition. **Song Liu:** Resources, Software. **Xu Wang**: Methodology, Project administration, Supervision, Validation. **Haitao Liu:** Supervision, Writing - review & editing. **Hao Song:** Investigation, Visualization, Data curation.

Declaration of competing interest

The authors declare that they have no known competing financial interests or personal relationships that could have appeared to influence the work reported in this paper.

Acknowledgement

This work was supported by Science and Technology R&D Plan Joint Fund of Henan Province (225200810052); China Postdoctoral Science Foundation (2020T130172); Key R & D and promotion projects of Henan Province (222102230064).

References

[1] Chen, Q.S. Mei, C.L. Li, L. Wan, H.H. Shao, J.Y. Li, X.M. Mei, Z.H. Chen, G.D. Zhang. Achieving a better combination of strength and electrical conductivity of Cu-Al_2O_3 nanocomposites by accumulative roll-bonding to ultrahigh cycles, Mater Charact. 178 (2021) 111205, https://doi.org/10.1016/j.matchar.2021.111205.

[2] P. Gaiser, M. Klingler, J. Wilde, The influence of strain hardening of copper on the crack path in Cu/Al_2O_3/Cu direct bonded copper substrates, Int J Fatigue. 140 (2020) 105821, https://doi.org/10.1016/j.ijfatigue.2020.105821.

[3] N. Simos, Z. Kotsina, E. Dooryhee, Z. Zhong, H. Zhong, F. Camino, E. Quaranta, N. Charitonidis, A. Bertarelli, S. Redaelli, L. Snead, D. Sprouster, 200 MeV proton irradiation of the oxide-dispersion-strengthened copper alloy (GlidCop-Al15), J. Nucl. Mater. 516(2019) 360-372, https://doi.org/10.1016/j.jnucmat.2019.01.026.

[4] X. Tan, K. Liu, Z.X. Wang, X.B. Yan, W.S. Yang, G.H. Wu, Mechanical behavior of deformable particles reinforced Al matrix composites, Mater. Sci. Eng. A. 806 (2021) 140815, https://doi.org/10.1016/j.msea.2021.140815.

[5] R. Kumar, A.K. Chaubey, S. Bathula, B.B. Jha, A. Dhar, Synthesis and characterization of Al_2O_3–TiC nano-composite by spark plasma sintering, Int. J. Refract. Met. Hard Mater. 54 (2016) 304-308, https://doi.org/10.1016/j.ijrmhm.2015.08.004

[6] F. Chen, Q.S. Mei, J.Y. Li, C.L. Li, L. Wan, X.M. Mei, Z.H. Chen, T. Xu, Y.C. Wang, Y.Y. Tan, Achieving synergistic strengthening and enhanced comprehensive properties of Cu matrix composites at high strength level by incorporating nanocarbons and Al_2O_3 dual reinforcements, Mater. Sci. Eng. A. 839 (2022) 142859, https://doi.org/10.1016/j.msea.2022.142859.

[7] D.S. Zhou, X.K. Wang, O. Muránsky, X.R. Wang, Y.H. Xie, C Yang, D.L. Zhang, Heterogeneous microstructure of an Al_2O_3 dispersion strengthened Cu by spark plasma sintering and extrusion and its effect on tensile properties and electrical conductivity, Mater. Sci. Eng. A. 730 (2018) 328-335, https://doi.org/10.1016/j.msea.2018.06.010.

[8] G. Dehm, C. Scheu, G. Möbus, R. Brydson, M. Rühle, Synthesis of analytical and high-resolution transmission electron microscopy to determine the interface structure of Cu/Al_2O_3, Ultramicroscopy. 67 (1997) 207-217, https://doi.org/10.1016/S0304-3991(97)00004-1.

[9] F. Chen, Q.S. Mei, C.L. Lia, L. Wan, H.H Shao, J.Y. Li, XM. Mei, Z.H. Chen, G.D. Zhang, Achieving a better combination of strength and electrical conductivity of Cu-Al_2O_3 nanocomposites by accumulative roll-bonding to ultrahigh cycles, Mater Charact. 178 (2021) 111205, https://doi.org/10.1016/j.matchar.2021.111205.

[10] I. Ahmad, M. Islam, S. Parvez, N. AlHabis, A. Umar, K. S. Munir, N.N. Wang, Y.Q. Zhu, Reinforcing capability of multiwall carbon nanotubes in alumina ceramic hybrid nanocomposites containing zirconium oxide nanoparticles, Int. J. Refract. Met. Hard Mater. 84 (2019) 105018, https://doi.org/10.1016/j.ijrmhm.2019.105018.

[11] X.F. Yu, H.D. Chen, G.Y. Liu, W.F. Li, H.Q. Liu, Study on cold deformability mechanical properties and uniformity of large round ODSC, Development and Application of Materials. 31 (2016) 61-65. https://doi.org/10.19515/j.cnki.1003-1545.2016.06.013.

[12] D.S. Zhou, X.K. Wang, O. Murnsky, X.R. Wang, Y.H. Xie, C. Yang, D.L. Zhang, Heterogeneous microstructure of an Al_2O_3 dispersion strengthened Cu by spark plasma sintering and extrusion and its effect on tensile properties and electrical conductivity, Mater. Sci. Eng. A. 730 (2018) 328-335, https://doi.org/10.1016/j.msea.2018.06.010.

[13] S.B. Chandrasekhara, S. Sudhakara Sarma, M. Ramakrishna, P. Suresh Babu, Tata N. Rao, B.P. Kashyap, Microstructure and properties of hot extruded Cu–1 wt% Al_2O_3 nano-composites synthesized by various techniques, Mater. Sci. Eng. A. 591 (2014) 46-53, http://dx.doi.org/10.1016/j.msea.2013.10.074.

[14] Y. Dong, X.K. Wang, Y.H. Xie, C. Yang, D.S. Zhou, Tunable microstructures and tensile mechanical properties of oxide-dispersion-strengthened Cu by extrusion and secondary processing, J. Alloys Compd. 812 (2020) 152112, https://doi.org/10.1016/j.jallcom.2019.152112.

[15] A. Mukhtara, D.L. Zhang, Mechanical behaviour of ultrafine grained Cu and Cu-(2.5 and 5) vol.%Al_2O_3 composites produced by powder compact forging, Adv Mat Res. 275 (2011) 170-173, https://doi.org/10.4028/www.scientific.net/AMR.275.170.

[16] Y.F. Zhang, Z. Ji, C.C. Jia, G.M. Liu, F.R Wan, Q. Zhan, Influence of La on enhancement of mechanical and electrical properties of Cu-Al_2O_3 composites, J. Rare Earths. 37 (2019) 534-540, https://doi.org/10.1016/j.jre.2018.08.016.

[17] Z.Y. Zhang, L.X. Sun, N.R. Tao, Raising thermal stability of nanograins in a CuCrZr alloy by precipitates on grain boundaries, J. Alloys Compd. 867 (2021) 159016, https://doi.org/10.1016/j.jallcom.2021.159016.

[18] Q. Zhao, Q. Lei, X.P. Gan, L. Zhang, K.C Zhou, Effects of the partially-unzipped carbon nanotubes on the microstructure and properties of CuCr matrix composites, Diamond Relat. Mater. 109 (2020) 108035, https://doi.org/10.1016/j.diamond.2020.108035.

[19] Z.W. Diao, F. Yang, R. Wang, Y. Zhang, L. Chen, T. Xiong, W. Yang, M.Z. Rong, Effect of heat treatment on the microstructure and properties of CuCrZr alloy manufactured by wire arc additive manufacturing, J. Alloys Compd. 967 (2023) 171786, https://doi.org/10.1016/j.jallcom.2023.171786.

[20] X.Z. Zhang, S.B. Jin, C Yang, D.S. Zhou, G. Sha, D.L. Zhang, Enhanced tensile properties in a Cu-Al_2O_3 alloy via trace Ti addition, J. Alloys Compd. 862 (2021) 158687,

https://doi.org/10.1016/j.jallcom.2021.158687.
[21] K.X. Song, J.D. Xing, Q.M. Dong, P. Liu, B.HH. Tian, X.J. Cao, Internal oxidation of dilute Cu–Al alloy powers with oxidant of Cu_2O, Mater. Sci. Eng. A. 380 (2004) 117-122, https://doi.org/10.1016/j.msea.2004.03.042.
[22] T. Baudin, A.L. Etter, R. Penelle, Annealing twin formation and recrystallization study of cold-drawn copper wires from EBSD measurements, Mater Charact. 58 (2007) 947-952, https://doi.org/10.1016/j.matchar.2006.09.009.
[23] A.L. Fan, S.K. Li, W.H. Tian, Grain growth and texture evolution in electroformed copper liners of shaped charges, Mater. Sci. Eng. A. 474 (2008) 208-213, https://doi.org/10.1016/j.msea.2007.04.001.
[24] C.D. Xia, W. Zhang, Z.Y. Kang, Y.L. Jia, Y.F. Wu, R. Zhang, G.Y. Xu, M.P. Wang, High strength and high electrical conductivity Cu–Cr system alloys manufactured by hot rolling–quenching process and thermomechanical treatments, Mater. Sci. Eng. A. 538 (2012) 295-301, https://doi.org/10.1016/j.msea.2012.01.047.
[25] L.Y. Shan, X.L. Wang, Y.L. Chang, Y.P. Wang, Improving the mechanical performance of Cu–Cr alloy by dissolving Cu in the Cr second phase, Mater Charact. 176 (2021) 111104, https://doi.org/10.1016/j.matchar.2021.111104.
[26] S. Sheibani, S. Heshmati-Manesh, A. Ataie, A. Caballero, J.M. Criado, Spinodal decomposition and precipitation in Cu–Cr nanocomposite, J. Alloys Compd. 587 (2014) 670-676, http://dx.doi.org/10.1016/j.jallcom.2013.11.019.
[27] S. Sheibani, S. Heshmati-Manesh, A. Ataie, Influence of Al_2O_3 nanoparticles on solubility extension of Cr in Cu by mechanical alloying, Acta Mater. 58 (2010) 6828-6834, http://dx.doi.org/10.1016/j.actamat.2010.09.012.
[28] S. Sheibani, A. Ataiea, S. Heshmati-Manesha, A. Caballero, J.M. Criado, Influence of Al_2O_3 reinforcement on precipitation kinetic of Cu–Cr nanocomposite, Thermochim Acta. 526(2011) 222-228, http://dx.doi.org/10.1016/j.tca.2011.09.024.
[29] Z. Savaedi, R. Motallebi, H. Mirzadeh, A review of hot deformation behavior and constitutive models to predict flow stress of high-entropy alloys, J. Alloy. Compd. 903 (2022) 163964, https://doi.org/10.1016/j.jallcom.2022.163964.
[30] X.X. Zhang, Y.L. Yuan, S.Q. Zhao, J. Zhang, Q.Z. Yan, Microstructure stability, softening temperature and strengthening mechanism of pure copper, CuCrZr and Cu-Al_2O_3 up to 1000 °C, Nucl. Mater. Energy. 30 (2022) 101123, https://doi.org/10.1016/j.nme.2022.101123.
[31] S.L. Tang, M. Zhou, Y. Zhang, D.Y. Xu, Z.Y. Zhang, X.H. Zheng, D. Li, X. Li, B.H. Tian, Y.L. Jia, Y. Liu, A.A. Volinskyf, E.S. Marchenko, Improved microstructure, mechanical properties and electrical conductivity of the Cu–Ni–Sn–Ti–Cr alloy due to Ce micro-addition, Mater. Sci. Eng. A. 871 (2023) 144910, https://doi.org/10.1016/j.msea.2023.144910.
[32] X.L. Wang, J.R. Li, Y. Zhang, Y.P. Wang, Improvement of interfacial bonding and mechanical properties of Cu-Al_2O_3 composite by Cr-nanoparticle-induced interfacial modification, J. Alloys Compd. 695 (2017) 2124-2130, http://dx.doi.org/10.1016/j.jallcom.2016.11.055.
[33] S. Han, K. Kim, J. Kang, H. Joh, S. Kim, J. Ahn, J. Lee, S. Lim, B. Han, Design of exceptionally strong and conductive Cu alloys beyond the conventional speculation via the interfacial energy-controlled dispersion of γ-Al_2O_3 nanoparticles, Sci. Rep. 5 (2015) 17364, https://doi.org/10.1038/srep17364.
[34] F. Long, X.H. Guo, K.X. Song, S.G. Jia, V. Yakubov, S.L. Li, Y.B. Yang, S.H. Liang, Synergistic strengthening effect of carbon nanotubes (CNT_s) and titanium diboride (TiB_2) microparticles on mechanical properties of copper matrix composites, J. Mater. Res. Technol. 9 (2020) 7989-8000, https://doi.org/10.1016/j.jmrt.2020.05.036.
[35] K.Y Duan, X.H. Guo, K.X. Song, X. Wang, J. Feng, S.L. Li, J.Y. Zhong, K. Li, Arc erosion resistance of WC/CuCr30 composites based on changing of Cr particle morphology and orientation, J. Mater. Res. Technol. 24 (2023) 9069-9081, https://doi.org/10.1016/j.jmrt.2023.05.116.
[36] L.C. Dong, B.F. Zhou, J. Zhong, Y.B. Zhong, T.X. Zheng, L.C. Dong, Y. Zhai, W.L. Ren, Z.S. Lei, Evolutions of the micro- and macrostructure and tensile property of Cu-15Ni-8Sn alloy during electromagnetic stirring-assisted horizontal continuous casting. Metall Mater Trans B. 50 (2019) 2111–2120, https://doi.org/10.1007/s11663-019-01664-3.
[37] L. Ren, W.L. Xiao, D. Kent, M. Wan, C. Ma, L. Zhou, Simultaneously enhanced strength and ductility in a metastable *β*-Ti alloy by stress-induced hierarchical twin structure, Scr. Mater. 184 (2020) 6-11, https://doi.org/10.1016/j.scriptamat.2020.03.039.
[38] H. Li, H.X. Zong, S.Z. Li, S.B. Jin, Y. Chen, M. J.Cabral, B. Chen, Q.W. Huang, Y. Chen, Y. Ren, K.Y. Yu, S. Han, X.D. Ding, G. Sha, J.S. Lian, X.Z. Liao, E. Ma, J. Sun, Uniting tensile ductility with ultrahigh strength via composition undulation. Nature. 604 (2022) 273–279, https://doi.org/10.1038/s41586-022-04459-w.
[39] Q.S. Pan, L.X. Zhang, R. Feng, Q.H. Lu, K. An, A.Chuang, J.D. Poplawsky, P.K. Liaw, L. Lul, Gradient cell–structured high-entropy alloy with exceptional strength and ductility. Science. 374 (2021) 984-989, https://doi.org/10.1126/science.abj8114.
[40] X.W. Feng, D.P. Zhang, B. Feng, Y.F. Lin, J. Wang, K.H. Zheng, Microstructure and properties of Cu-0.4 wt.%Al_2O_3 composites fabricated by hot extrusion and cold drawing, J. Mater. Eng. Perform. 31 (2022) 1241-1249, https://doi.org/10.1007/s11665-021-06247-5
[41] T.J. Jang, W.S. Choi, D.W. Kim, G. Choi, H. Jun, A. Ferrari, F. Krmann, P. Choi, S. Sohn, Shear band-driven precipitate dispersion for ultrastrong ductile medium-entropy alloys, Nat. Commun. 12 (2021) 4703,

https://doi.org/10.1038/s41467-021-25031-6
[42] H.R. Lin, X.H. Guo, K.X. Song, S.L. Li, J. Feng, X.F. Zhang, M.Q. Feng, Synergistic strengthening effect of tungsten carbide (WC) particles and silicon carbide whiskers (SiC_w) on mechanical properties of Cu-Al_2O_3 composite, J. Mater. Res. Technol. 15 (2021) 2837-2 847, https://doi.org/10.1016/j.jmrt.2021.09.103.
[43] F. Long, X.H. Guo, K.X. Song, J.Q. Liu, X. Wang, Y.B. Yang, S.L. Li, An internal-oxidation-based strategy induced high-density alumina in-situ nanoprecipitation and carbon nanotube interface optimization for co-reinforcing copper matrix composites, Compos. B. Eng. 229 (2022) 109455, https://doi.org/10.1016/j.compositesb.2021.109455.
[44] C.G. Li, Y.H. Xie, D.S. Zhou, W. Zeng, J. Wang, J.M. Liang, D.L. Zhang, A novel way for fabricating ultrafine grained Cu-4.5 vol.%Al_2O_3 composite with high strength and electrical conductivity, Mater Charact. 155 (2019) 109775, https://doi.org/10.1016/j.matchar.2019.06.017.
[45] Y.C. Zhang, C.H. Chen, J. Xiong, Z.X. Guo, J.B. Liu, Q.B. You, L. Yang, D.J. Zhang, Y. Liu, Q. Liu, X.Q. Jia, Effects of nano-Al_2O_3 addition on microstructure, mechanical properties, and wear resistance of Ti(C, N)-based cermets, Int. J. Refract. Met. Hard Mater. 115 (2023) 106290, https://doi.org/10.1016/j.ijrmhm.2023.106290.
[46] J. Lee, Y.C. Kim, S. Lee, S. Ahn, N.J. Kim, Correlation of the microstructure and mechanical properties of oxide-dispersion-strengthened coppers fabricated by internal oxidation, Metall Mater Trans A. 35 (2004) 493–502, https://doi.org/10.1007/s11661-004-0360-9.